A compact holographic optics-based interferometer

A. K. Aggarwal*, Sushil K. Kaura, D. P. Chhachhia and A. K. Sharma

Coherent Optics Division, Central Scientific Instruments Organization, Sector 30, Chandigarh 160 030, India

A compact holographic optics-based interferometer involving the use of minimal bulk optical components is described. The optical arrangement in the proposed system involves a simple alignment procedure, and conventional holographic recording material is used in the formation of holographic optical elements. Recording schemes for the formation of holographic optical elements and related techniques for the realization of the proposed interferometer along with typical experimental results are presented. The interferometer is quite suitable for performing optical test studies on phase (transparent) objects in real time.

OPTICAL test techniques are increasingly finding use in various precision-measurement-related fields. Several kinds of optical test studies have been performed using different types/configurations of optical interferometers[1]. There is one class of interferometers that directly maps the aberrated wavefront, such as Twyman–Green and Mach–Zehnder interferometers in which the aberrated wavefront is made to interfere with a reference wavefront. There is another class of shearing interferometers in which the aberrated wavefront is made to interfere with a replica of itself, after it has been sheared by some amount in some direction. The conventional optical interferometers generally use expensive, precise, custom-made, bulky optics and also involve rather tedious and time-consuming alignment procedures, which make them impractical in some applications. The use of holographic optical elements instead of conventional optics can drastically reduce the bulkiness and high cost factors. Because of the several attractive features offered by holographic optical elements (HOEs), such as light weight; compactness; ease of fabrication; containing multiple optical functions in the single element, their use provide the advantage in the construction of compact optical systems. The replacement of conventional optics with HOEs can drastically reduce the bulkiness, high cost factors and provide the optical systems with improved functionality. HOEs are increasingly finding their applications for performing various kinds of optical test studies[2–5] and also in several specialized applications[6,7]. The applications of HOEs have, however, been largely reported in the area of shearing interferometry[8–10]. In recent years, there has been a renewed interest in using optical interferometers for carrying out phase visualization and measurement studies[11–15]. In this communication, we describe a simple method for making a compact holographic optics-based interferometer, which is suitable for performing optical test studies of phase (transparent) objects in real time.

The method reported here is based on the formation of three holographic optical elements separately, in two recording steps, on two different recording plates (Figure 1). For the formation of these three holographic optical elements, the upper, lower and middle portions of a collimated beam (labelled as object beams O_1, O_2 and O_3 respectively) are used separately. The first recording step of the method involves the formation of two spatially separated holographic optical elements (HOE_1 and HOE_2) on the first recording plate (H_1), where HOE_1 is formed by using O_1 in conjunction with another collimated beam (labelled as reference beam R_1) and HOE_2 is formed by using O_2 in conjunction with a second collimated beam (labelled as reference beam R_2). These two permanently recorded holographic optical elements on H_1 provide two inbuilt[16] collimated beams for subsequent recording. In the second recording step of the method, diffracted-order of beams R_1 and R_2 (which are the replica of R_1 and R_2 respectively) are generated from HOE_1 and HOE_2 with the illuminating beams O_1 and O_2 respectively. The so-generated beams R_1 and R_2 are used independently, in two separate holographic exposures, in conjunction with the common beam O_3 for the formation of two different but overlapped holographic optical elements on the second recording plate (H_2). After processing, H_2 is repositioned at the same location at which it was recorded. These two holographic plates (H_1 and H_2), when placed in this configuration and illuminated with the beams O_1 and O_2 (where beam O_3 is blocked by a stopper (ST)), serve as a versatile two-beam interferometer (Figure 2). Here HOE_1 and HOE_2 (formed on the plate H_1), upon illumination with the beams O_1 and O_2 respectively, provide two different illuminating beams R_1 and R_2 for H_2. H_2 is thereafter illuminated with the so-generated illuminating beams R_1 and R_2. These two illuminating beams (R_1 and R_2) further provide from H_2, two diffracted-order of beam

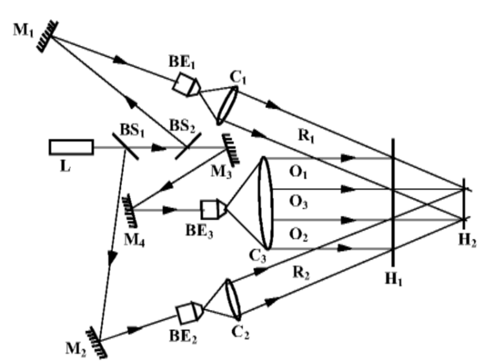

Figure 1. Recording scheme for generation of holographic optical elements for the formation of the interferometer.

*For correspondence. (e-mail: aka1945@rediffmail.com)

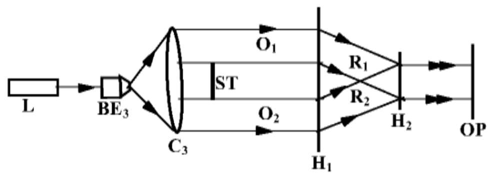

Figure 2. Schematic of a compact holographic optics-based interferometer.

O_3 (which are a replica of O_3) overlapping each other. The portion of any one of the two collimated beams generated between H_1 and H_2 can be used as a test arm. Repositioning of H_2 results in a finite-fringe interferogram, which, with a careful alignment procedure, would yield an infinite-fringe interferogram. In this setting, optical test studies on a phase (transparent) object can be performed in real-time by placing it in any one of the test arms.

The complex amplitude distribution of the three object-plane wavefronts and the two reference-plane wavefronts can be considered as O_1, O_2, O_3 and R_1, R_2 respectively. The resultant intensity at the recording plate H_1 is given by[17]

$$I = |O_1 + R_1|^2 + |O_2 + R_2|^2. \tag{1}$$

The amplitude transmittance of the processed H_1 is

$$t_1 \sim |O_1 + R_1|^2 + |O_2 + R_2|^2. \tag{2}$$

For the formation of two different and overlapped holographic optical elements on H_2, HOE_1 and HOE_2 (formed on plate H_1) are illuminated with beams O_1 and O_2 respectively (as was used in the first recording step). The complex amplitude of the transmitted field from H_1 is

$$\begin{aligned} U_1 &\sim O_1[|O_1 + R_1|^2] + O_2[|O_2 + R_2|^2] \\ &\sim O_1|O_1|^2 + R_1|O_1|^2 + O_1^2R_1^* + O_1|R_1|^2 + O_2|O_2|^2 \\ &+ R_2|O_2|^2 + O_2^2R_1^* + O_2|R_2|^2. \end{aligned} \tag{3}$$

We can consider $|O_1|^2$ and $|O_2|^2$ to be constant across H_1, as plane beams O_1 and O_2 are used for the illumination of HOE_1 and HOE_2 respectively, on plate H_1. Thus, only the 2nd and 6th terms on the right-hand side of eq. (3) are of interest to us, as they represent the diffracted-order of beams R_1 and R_2 (which are the replica of the original reference beams R_1 and R_2 respectively), i.e.

$$\begin{aligned} &|O_1|^2R_1 + |O_2|^2R_2 \\ &\quad = \text{Constant. } R_1 + \text{Constant. } R_2. \end{aligned} \tag{4}$$

These two generated reference beams (R_1 and R_2) are further used independently in two separate holographic exposures, in conjunction with a common collimated beam O_3 for the formation of two different but overlapped holographic optical elements on H_2 in the second recording step. After processing, H_2 is repositioned at the same location at which it was recorded. The amplitude transmittance of the processed H_2 is

$$t_2 \sim |R_1 + O_3|^2 + |R_2 + O_3|^2. \tag{5}$$

In this configuration, when HOE_1 and HOE_1 (formed on plate H_1) are illuminated with beams O_1 and O_2 respectively, they provide illuminating beam R_1 (from HOE_1) and R_2 (from HOE_2) for the two independently recorded holographic optical elements on H_2. The complex amplitude of the transmitted field from H_2 is

$$\begin{aligned} U_2 &\sim R_1[|R_1 + O_3|^2] + R_2[|R_2 + O_3|^2] \\ &\sim R_1[|R_1|^2 + |O_3|^2] + R_2[|R_2|^2 + |O_3|^2] + |R_1|^2O_3 \\ &+ |R_2|^2O_3 + R_1^2O_3^* + R_2^2O_3^*. \end{aligned} \tag{6}$$

In the right-hand side of eq. (6), the first term represents the undiffracted-order of beam R_1 and the second term represents the undiffracted-order of beam R_2. Similarly, the third term represents the diffracted-order of beam O_3 (generated due to R_1 illuminating beam) and the fourth term represents the diffracted-order of beam O_3 (generated due to R_2 illuminating beam) and is overlapping the above diffracted-order of beam O_3. These two beams thus provide two overlapped interfering beams in the observation plane OP (Figure 2). A typical finite-fringe interferogram obtained in the observation plane with this set-up is given in Figure 3 *a*. By applying a simple alignment procedure in repositioning of H_2, results in an infinite-fringe interferogram (Figure 3 *b*) in the observation plane. In this configuration, portion of any one of the two collimated beams, generated between H_1 and H_2, can be used as a test arm for performing optical test studies on phase (transparent) objects. Typically, if a phase object $S = \exp[i\phi]$ is introduced in one of the test arm, say R_2, then the complex amplitude of the transmitted field from H_2 (containing two independently recorded holographic optical elements) is given by

$$\begin{aligned} U_3 &\sim R_1[|R_1 + O_3|^2] + R_2S[|R_2 + O_3|^2] \\ &\sim R_1[|R_1|^2 + |O_3|^2] + R_2S[|R_2|^2 + |O_3|^2] + |R_1|^2O_3 \\ &+ |R_1|^2O_3S + R_1^2O_3^* + R_1^2O_3^*S. \end{aligned} \tag{7}$$

In the right-hand side of eq. (7), the third term represents the diffracted-order of beam O_3 (generated due to R_1 illuminating beam) and the fourth term represents the diffracted-order of beam O_3 (generated due to R_2S illuminating beam). The amplitude transmittance due to these two overlapped interfering beams is

$$U_4 \sim |R_1|^2O_3 + |R_2|^2O_3S.$$

The intensity distribution of the interference pattern in the observation plane is

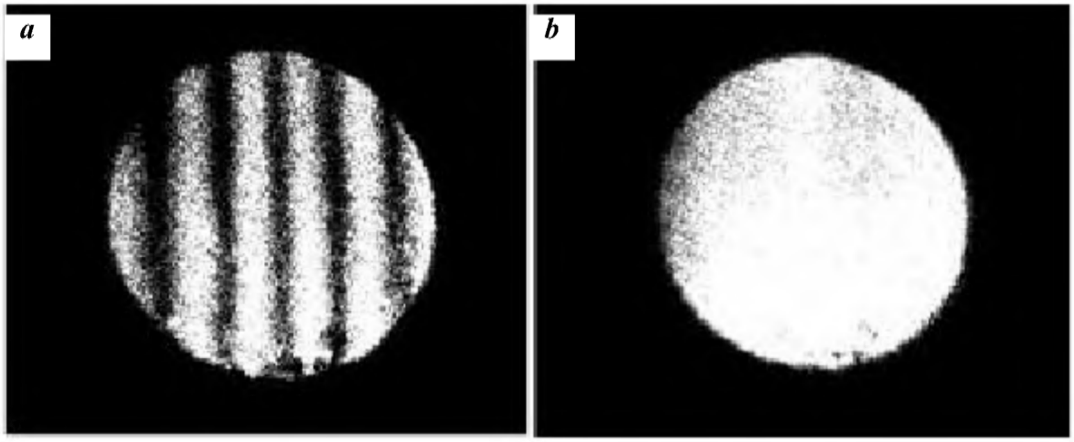

Figure 3. Photograph of (***a***) finite-fringe interferogram and (***b***) infinite-fringe interferogram.

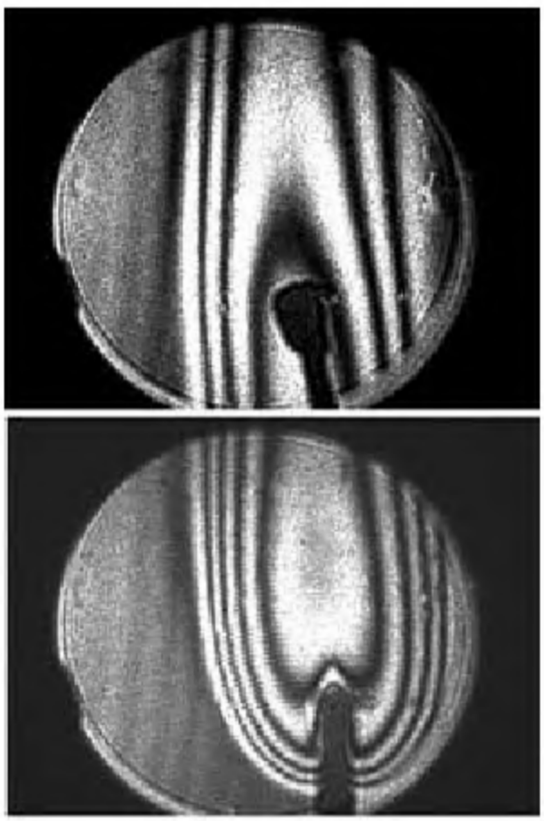

Figure 4. Photograph of interference pattern of heat flow obtained by inserting a burning matchstick in the test arm.

$$I_r \sim U_4 U_4^*$$
$$\sim |O_3|^2|R_1|^4 + |R_2|^4|O_3|^2|S|^2 + |R_1|^2|R_2|^2|O_3|^2(S + S^*).$$
$$I_r \sim A + B\cos\phi, \tag{8}$$

where A and B are constants. It is thus seen that the intensity distribution of the interference pattern, recorded in the observation plane, depends only on the phase variation introduced by the phase object (S) into the test arm (R_2) between H_1 and H_2.

In our experimental arrangement (Figure 1), a 3 mW He–Ne laser system was used in the first and second recording steps of the method for the formation of H_1 and H_2. Light from the laser (L) is split by a variable beam splitter (BS_1) into two components. The transmitted component is further split into two components by another variable beam splitter (BS_2). The transmitted and reflected components from BS_2 are used for the generation of object beams (O_1, O_2 and O_3) and reference beam (R_1) respectively. The reflected component from BS_1 is used for the generation of another reference beam (R_2). Collimated reference beams (R_1 and R_2) are generated through beam expanders (BE_1 and BE_2) in conjunction with 30 mm diameter-collimating lenses (C_1 and C_2 respectively). Collimated object beam is generated through a beam expander (BE_3) in conjunction with a 100 mm diameter collimating lens (C_3). The upper and lower portions (O_1 and O_2) of the object beam are used separately for the formation of two spatially separated holographic optical elements on H_1 in the first recording step. The middle portion (O_3) of the object beam is used separately for the formation of two different but overlapped holographic optical elements, involving two separate holographic exposures, on H_2 in the second recording step. The shear plate interferometric technique was applied to ensure the optical quality of the collimated beams, which were used for forming the holographic optical elements on H_1 and H_2. Standard Kodak D-19 developer and R-9 bleach bath solutions are used for Agfa-Gevaert 8E75HD plates (having spatial resolution power of more than 3000 mm^{-1}) to give high efficiency and low noise grating holograms. Holographic optical elements with almost uniform diffraction efficiency were generated using these holographic recording plates with exposure energies of the order of 160–180 $\mu J/cm^2$. It is to be noted that in order to realize the proposed

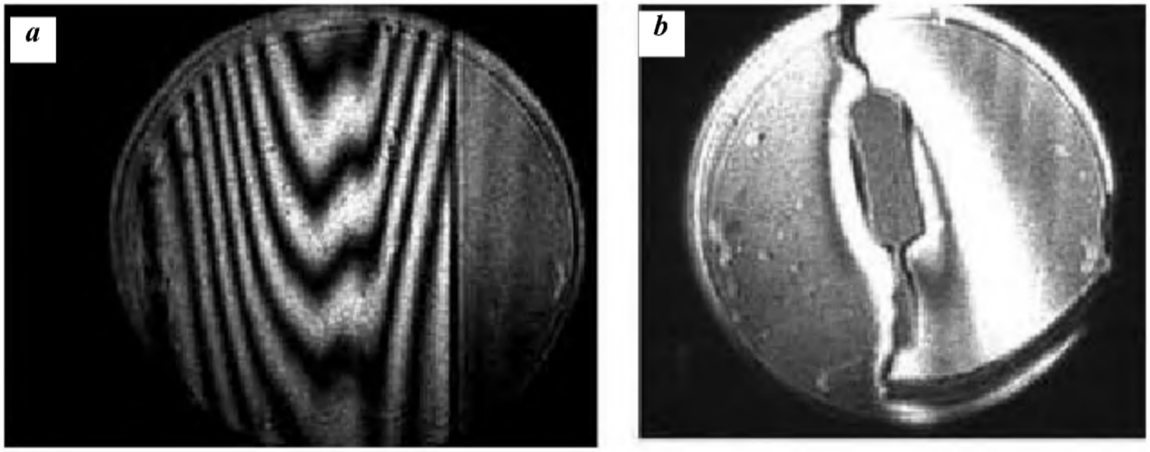

Figure 5. Photograph of interference pattern of heat flow obtained by inserting (***a***) a microscope cover slide plate and (***b***) an active electronic resistor in the test arm.

interferometer set-up, the processed H_2 plate is required to be repositioned at the same location at which it was formed.

Normally, one can accomplish it by performing an *in situ* processing of the exposed H_2 plate or by employing a tedious and time-consuming/cumbersome alignment procedure. However, since in our recording scheme the respective interfering beams used for the formation of holographic optical elements on both H_1 and H_2 plates have permanently been frozen, repositioning became much simpler. We could achieve it by merely mounting the H_2 plate on a holder having the capabilities of providing tilt motion to the plate in horizontal and vertical directions. Using a simple alignment procedure, an infinite-fringe interferogram is easily obtained in the observation plane. Optical test studies on phase objects were performed by inserting them in either of the test arms (R_1 or R_2) between H_1 and H_2. Figure 4 shows a typical interference pattern due to heat flow of a burning matchstick. The optical arrangement with this method is quite suitable for performing optical test studies on phase objects in real time. The optical quality of a microscope cover slide plate was tested by inserting it in one of the test arms and the typical interference pattern obtained is given in Figure 5 *a*. Figure 5 *b* shows a typical interference pattern in real time due to heat flow from an active electronic resistor. The results presented here have been captured frame-by-frame to show the versatility of the proposed interferometer. Using hologram-copying techniques[18], holographic copies of H_1 and H_2 can be generated in large numbers that can further facilitate the production of cost-effective, simple and compact, holographic, optics-based interferometers.

We have described a simple method for making a compact, holographic, optics-based interferometer, which is suitable for performing optical test studies on phase (transparent) objects. The advantage of this method lies in the fact that the proposed optical arrangement of the interferometer involves a simple alignment procedure and a portion of either of the collimated beams (i.e. R_1 or R_2) generated between H_1 and H_2 can be used as a test arm for studying the phase objects. It may be seen from Figures 4 and 5 that this interferometric method, in infinite-fringe mode set-up, gives high-contrast interference patterns on insertion of a phase object in any one of the two test arms. Quantitative evaluation of the phase change may be performed by phase-shifting interferometry. It is possible to acquire a series of interferograms from this interferometer by introducing an arbitrary phase delay in a series of steps using suitable optical elements (e.g. quarter-wave plate, half-wave plate, etc.) between the reference and the test waves, without varying the physical lengths of the optical paths. Wavefront distortions caused due to emulsion shrinkage/swelling and substrate, etc. get cancelled as both the interfering beams pass through the same portion of H_2. This interferometric method, in infinite-fringe mode set-up, facilitates studies of phase objects in real time. Further, the described geometry of the interferometer is simple and can be realized with relative ease, and the vital components of the interferometer could be produced in great numbers using hologram-copying methods.

1. Malacara, D. (ed.), *Optical Shop Testing*, Wiley, New York, 1992, 2nd edn, pp. 51–206.
2. Kitchen, S. R. and Hansen, C. D., Holographic common-path interferometer for angular displacement measurements with spatial phase stepping and extended measurement range. *Appl. Opt.*, 2003, **42**, 51–59.
3. Hanson, S. G., Lindvold, L. R. and Hansen, B. H., Robust optical systems for non-destructive testing based on laser diodes and diffractive optical elements. *Opt. Lasers Eng.*, 1998, **30**, 179–189.
4. Chen, C. W. and Breckinridge, J. B., Holographic Twymann–Green interferometer. *Appl. Opt.*, 1982, **21**, 2563–2568.
5. Castaneda, J. O., Jara, E. and Ibarra, J., Holographic interferometer with tunable radial and lateral displacement. *Appl. Opt.*, 1990, **29**, 949–952.

6. Goodman, J. W. (ed.), *International Trends in Optics*, Academic Press, New York, 1991, pp. 57–110.
7. Widmann, K., Pretzler, G., Woisetschlager, J., Neger, T. and Jager, H., Application of holographic optical elements to plasma diagnostics. *SPIE*, 1992, **1732**, 712–718.
8. Matsuda, K., Minami, Y. and Eiju, T., Novel holographic shearing interferometer for measuring lens lateral aberration. *Appl. Opt.*, 1992, **31**, 6603–6609.
9. Joenathan, C., Parthiban, V. and Sirohi, R. S., Shear interferometry with holographic lenses. *Opt. Eng.*, 1987, **26**, 359–364.
10. Shakher, C., Godbole, P. B. and Gupta, B. N., Shearing interferometry using hololenses. *Appl. Opt.*, 1986, **25**, 2477–2479.
11. Anderson, C. S., Fringe visibility, irradiance and accuracy in common path interferometers for visualization of phase disturbances. *Appl. Opt.*, 1995, **34**, 7474–7485.
12. Ferrari, J. A. and Frins, E. M., One-beam interferometer by beam folding. *Appl. Opt.*, 2002, **41**, 5313–5316.
13. Aggarwal, A. K. and Kaura, S. K., Further application of point diffraction interferometer. *J. Opt.* (*Paris*), 1986, **17**, 135–138.
14. Ferrari, J. A., Frins, E. M., Perciante, D. and Dubra, A., Robust one-beam interferometer with phase-delay control. *Opt. Lett.*, 1999, **24**, 1272–1274.
15. Zeilikovich, I. S. and Platonov, E. M., Interferometer with holographic optics. *Opt. Laser Technol.*, 1985, **17**, 145–147.
16. Aggarwal, A. K. and Kaura, S. K., Rainbow holograms with an inbuilt reference beam. *J. Opt.* (*Paris*), 1987, **18**, 63–66.
17. Hecht, E. and Zajac, A., *Optics*, Addison-Wesley, Reading, Mass., 1974.
18. Caulfield, H. J. (ed.), *Handbook of Holography*, Academic Press, New York, 1979, pp. 373–378.

ACKNOWLEDGEMENTS. We are grateful to Dr R. P. Bajpai, Director, Central Scientific Instruments Organization, Chandigarh for constant encouragement, support and permission to publish this work. We thank Department of Science and Technology, New Delhi for financial support. A.K.S. thanks CSIR, New Delhi for a fellowship. We also thank Mr H. K. Sardana and Mr H. N. Bhargaw for help in recording the experimental results.

Received 2 January 2004; revised accepted 25 March 2004

Theoretical design for a light-driven molecular motor based on rotaxanes

K. L. Sebastian

Department of Inorganic and Physical Chemistry, Indian Institute of Science, Bangalore 560 012, India

We suggest a design for a light-driven molecular motor, which is different from the existing designs. It is a rotaxane molecule, having identical 'stations' and an asymmetric 'shuttle'. We argue that the molecule would exhibit unidirectional rotational/translational motion continuously, upon shining with light of just one frequency. With this design, it should be possible to synthesize a light-driven single-molecular motor in the near future.

e-mail: kls@ipc.iisc.ernet.in

THERE has been considerable interest in the design and fabrication of molecular devices[1–16]. Of particular interest are molecular motors in which the components are forced to move past each other by external stimuli[1–11]. Recent insights into the working of biological motors[10,17,18] have stimulated a surge of papers on such artificial molecular motors. Rotaxanes are the most widely studied as they offer the possibility of long range translational motion of a threaded 'shuttle' along a molecular wire or 'rail track'. The shuttle can be driven chemically, electrochemically or photochemically.

Natural molecular motors are usually driven by chemical energy and are believed to have high efficiency, often close to unity. One of the most efficient natural motors, the ATP synthase, rotates 15–20 times per second. Though chemically driven motors are plentiful in biology, their components are rather largish molecules and it does not look as if an artificial molecular motor of comparable efficiency satisfying the three desirable features will be made in the near future. Any synthetic molecular motor should have the following desirable characteristics: (a) It should draw energy from a source and produce mechanical work, with high efficiency, hopefully comparable to those of natural molecular motors. (b) The motion produced should be on a time scale, faster or at least comparable to those of natural molecular motors. (c) Its operation should not, if possible, lead to the formation of waste products.

In an interesting paper, unidirectional rotational motion in a mechanically interlocked catenane molecule has been reported[8]. The authors have studied a 'three-station' [2]catenane and a 'four-station' [3]catenane. 'Stations' are the binding sites in the macrocyclic ring of the catenane assembly. In these systems, there is a large macrocycle with the binding sites and smaller macrocyles which are bound to these sites. It was found that in response to external stimuli, the small ring in the three-station [2]catenane moves sequentially between the binding sites. In the four-station [3]catenane there are two smaller macrocycles and one of them blocks the backward Brownian movement of the other macrocycle, effectively making the rotation unidirectional.

The chemically driven motors that have been synthesized recently[1–8] are of great interest, though they have rather low efficiency and rotate by 360 degrees on a rather long time scale (for example, one day). They are in no way near the goals that one would like to achieve. The existing attempts based on rotaxanes have not put the ideas from Brownian motors to maximum use to get an efficient molecular motor.

Here, we suggest a design that we believe will lead to machines that satisfy all the three requirements above. It is to be stressed that the ideas that we use are well known